

Phase diagram for $\text{Ca}_{1-x}\text{Y}_x\text{MnO}_3$ type crystals.

H. Aliaga, R. Allub* and B. Alascio*

Centro Atómico Bariloche, (8400) S. C. de Bariloche, Argentina.

Abstract

We present a simple model to study the electron doped manganese perovskites. The model considers the competition between double exchange mechanism for itinerant electrons and antiferromagnetic superexchange interaction for localized electrons. It represents each Mn^{4+} ion by a spin $1/2$, on which an electron can be added to produce Mn^{3+} ; we include a hopping energy t , a strong intratomic interaction exchange J (in the limit $J/t \rightarrow \infty$), and an interatomic antiferromagnetic interaction K between the local spins.

Using the Renormalized Perturbation Expansion and a Mean Field Approximation on the hopping terms and on the superexchange interaction we calculate the free energy. From it, the stability of the antiferromagnetic, canted, , ferromagnetic, and novel spin glass phases can be determined as functions of the parameters characterizing the system.

The model results can be expressed in terms of t and K for each value of the doping x in phase diagrams.

The magnetization m and canting angle θ can also be calculated as functions of temperature for fixed values of doping and model parameters.

Keywords: A. magnetically ordered materials D. electronic transport

*Member of the Carrera del Investigador Científico del Consejo Nacional de Investigaciones Científicas y técnicas (CONICET).

I. INTRODUCTION

The discovery of 'colossal' magnetoresistance (CMR) in $\text{La}_{1-x}\text{Sr}_x\text{MnO}_3$ type compounds [1] together with its many unusual properties have attracted considerable attention. The phase diagram, as a function of concentration x , temperature, magnetic field, or magnitude of the superexchange interaction is not quite clear yet for the different compounds.

Before the discovery of CMR, Jonker and Van Santen [2] established a temperature-doping phase diagram separating metallic ferromagnetic from insulating antiferromagnetic phases. Zener [3] proposed a 'Double Exchange' (DE) mechanism to understand the properties of these compounds and the connection between their magnetic and transport properties. This DE mechanism was used by Anderson and Hasegawa [4] to calculate the ferromagnetic interaction between two magnetic ions, and by de Gennes [5] to propose canting states for the weakly doped compounds. Kubo and Ohata [6] used a spin wave approach to study the temperature dependence of the resistivity at temperatures well below the critical temperature and a mean field approximation at T near T_c . Mazzaferro, Balseiro and Alascio [7] used a mixed valence approach similar to that devised for TmSe combining DE with the effect of doping to propose the possibility of a metal insulator transition in these compounds.

Since [1], a wealth of experimental results have been obtained on the transport, optical, spectroscopic and thermal properties of these materials under the effects of external magnetic fields and pressures [8].

Theoretically, Furukawa [9] has shown that DE is essential to the transport theory of these phenomena, while Millis *et al.* [10] have argued that DE alone is not sufficient to describe the properties of some of the alloys under consideration and have proposed that lattice polaronic effects play an important role. In a previous paper we have shown that a semi-phenomenological model, that includes the effect of the disorder introduced by doping, can explain the transport properties of $\text{La}_{1-x}\text{Sr}_x\text{MnO}_3$ [11].

In [11] we treat the Hamiltonian proposed for these systems using an alloy analogy approximation to the exchange terms and including the effects of disorder by introducing a

continuous distribution of the diagonal site energies. Since the focus of the paper was on transport properties of the ferromagnetic materials, we emphasize the disorder aspects of the problem and ignore interactions that would give rise to phases other than ferromagnetic.

Here we propose to extend the previous studies to the region of concentration of dopant where the antiferromagnetic interactions, always present, compete with double exchange. We will focus on the Ca rich end of $(\text{RE})_x\text{Ca}_{1-x}\text{MnO}_3$ compounds (where RE stands for rare earths) because the antiferromagnetic order is simpler in these alloys.

We include from the start antiferromagnetic interactions between nearest neighbors, which we treat in mean field approximation. To simplify the problem we start in this paper by ignoring disorder effects to study the stability of different phases.

In Section II, we set up the model Hamiltonian and we explain some approximations which we use in order to solve the model.

Finally, Section III is devoted to obtain the Green's functions relevant to calculate the kinetic energy of the model, and then we formulate a free energy that allows us to obtain the different magnetic phases. We discuss their physical implications and show the results for the density of states and critical temperatures phase diagrams.

II. MODEL

The System in consideration contains two kinds of magnetic ions:

Mn^{4+} with three localized t_{2g} electrons giving rise to a spin $3/2$. We will refer to this electrons as the 'localized spin' electrons.

Mn^{3+} , which besides the localized spin, contains an itinerant electron in the ϵ_g orbitals. Due to the strong intra atomic exchange coupling J , this ϵ_g electron couples ferromagnetically to the localized spin to produce a spin two at these sites.

The itinerant electron can jump conserving spin from site to site with hopping energy t . These processes give rise to the double exchange mechanism making the system transport properties metallic like and trying to order the spins ferromagnetically. It is easy to estimate

the energy gain in the ferromagnetic state due to this process as being of the order of the hopping energy t times the doping x .

Superexchange between localized spins gives rise to an antiferromagnetic coupling K that competes with double exchange and can lead to different phases. We investigate here the stability of canted, ferro and antiferromagnetic phases. To this end, we divide the Mn lattice in two interpenetrating sublattices appropriate to describe type G antiferromagnetism [12] which is known to be stable at the Ca rich end of the composition. We indicate by I or II the sites belonging to each sublattice, and define a quantization axis for each sublattice.

According to the above considerations we write the following model Hamiltonian:

$$H = \sum_{i,\sigma} \varepsilon_i \cdot n_{i,\sigma} + U \sum_{i,\sigma} n_{i,\sigma} \cdot n_{i,-\sigma} + J \sum_i \mathbf{S}_i \cdot \sigma_i + K \sum_{\langle i,j \rangle} \mathbf{S}_i \cdot \mathbf{S}_j + \sum_{\langle i,j \rangle, \sigma} t_{ij} \left(c_{i\sigma}^+ \cdot c_{j\sigma} + h.c. \right) \quad (1)$$

where $n_{i,\sigma} = c_{i\sigma}^+ c_{i\sigma}$, and $c_{i\sigma}^+$, $c_{i\sigma}$ creates and destroys an itinerant electron with spin σ at site i , respectively. \mathbf{S}_i and σ_i are the localized and itinerant spin operators at site i , respectively. ε_i are the site diagonal energies, U is the intra-atomic electronic repulsion, and t_{ij} is the hopping parameter between nearest neighbors sites i, j .

In order to reduce the complexity of the mathematical treatment, we make from the start two simplifying assumptions that will be discussed later: we neglect spin flip processes between itinerant and localized electrons (i.e. keep only the z component of the $\mathbf{S}_i \cdot \sigma_i$ interaction) and use a mean field approximation to the antiferromagnetic interaction (i.e. we replace $\mathbf{S}_i \cdot \mathbf{S}_j$ by $S_{z,i} \cdot \langle S_{z,j} \rangle + S_{z,j} \cdot \langle S_{z,i} \rangle - \langle S_{z,j} \rangle \cdot \langle S_{z,i} \rangle$).

After doing this, the Hamiltonian can be separated into a local H_0 and a non-local H_1 .

$$H = H_0 + H_1 \quad (2)$$

where:

$$H_0 = \sum_{i,\sigma} \varepsilon_i \cdot n_{i,\sigma} + U \cdot \sum_{i,\sigma} n_{i,\sigma} \cdot n_{i,-\sigma} + J \cdot \sum_i S_{z,i} \cdot \sigma_{z,i} + K \cdot \sum_i S_{z,i} \cdot \sum_j \langle S_{z,j} \rangle \quad (3)$$

and

$$H_1 = \sum_{\langle i,j \rangle, \sigma} t_{ij} (c_{i\sigma}^+ \cdot c_{j\sigma} + h.c.) \quad (4)$$

In order to reduce the mathematical complexity of the problem to a minimum we make the following additional simplifications:

a) We represent the localized spin to be $1/2$, so that they can be parallel or antiparallel to the local quantization direction on each sublattice.

b) We take the semiclassical approximation for the hopping energy: $t_{ij} = t \cdot \cos(\theta)$, where θ is halve the angle between localized spin directions in I and II sublattices.

c) the diagonal energies ε_i are all equal and define the zero of one-particle energies. Chemical disorder, which is present in real samples and fundamental to the transport properties, is ignored in this first approach. The effect of disorder in the thermodynamic properties is not crucial to the ordered phases and can be estimated at large disorder by replacing the hopping energy t by (t^2/Γ) where Γ measures the width of the energy distribution [13].

d) Coulomb repulsion U and exchange J are much larger than t_{ij} and taken to be infinite here. Finite U and J lead to effective antiferromagnetic coupling between Mn^{3+} ions and compete in the La rich side of the alloys with the ferromagnetic coupling due to double exchange. The large U limit precludes occupation of the ϵ_g orbitals at each site by more than one itinerant electron.

e) We ignore lattice dynamics that could give rise to polaronic effects. This phenomena have been discussed by [10] and references therein. When necessary, they may be included a posteriori.

III. RESULTS AND DISCUSSION

In order to obtain the density of states for itinerant electrons, we have to calculate local Green's functions. To obtain the local Green's functions, we resort to the same procedure as in [11] and [7] and work on a interpenetrating Bethe lattice. The itinerant electrons spin up Green's functions corresponding to H_0 at a local spin up site is given by

$$G_{i\uparrow\alpha}^{0l} = \langle\langle c_{i\uparrow}; c_{i\uparrow}^\dagger \rangle\rangle = \frac{[\omega - E_\alpha - U(1 - \bar{n}_{i\downarrow})]}{(\omega - E_\alpha)(\omega - E_\alpha - U)}, \quad (5)$$

where $\bar{n}_{i\downarrow} = \langle c_{i\downarrow}^\dagger c_{i\downarrow} \rangle$, $\alpha = + (-)$ for up (down) localized spin, l is the sublattice index (I, II), and $E_\alpha = \epsilon - \alpha J$, which for large J and U reduces to

$$G_{i\uparrow\alpha}^{0l} = \frac{\delta_{\alpha+}}{\omega - \epsilon + J}, \quad (6)$$

at the lowest energy pole, which from here on we take at zero ($\epsilon = J$).

The Renormalized Perturbation Expansion (RPE) [16] as in [11] connects the propagator at site i to propagators at the nearest neighbor sites $i + \delta$ which exclude visiting site i again and which we will denote by small g 's. These new propagators are in turn connected to propagators of the same type at sites $i + \delta + \delta'$ etc., so that the Green function at each site depends through this chain on local spin configuration because of the factors $\delta_{\alpha+}$.

The defined chain of equations read for example:

$$G_{i\uparrow+}^I = \frac{1}{\omega - \Delta_{i\uparrow}^{I+}}, \quad (7)$$

where the self energy $\Delta_{i\uparrow}^{I+}$ is

$$\Delta_{i\uparrow}^{I+} = \sum_{\delta} t_{i,i+\delta}^2 g_{i+\delta\uparrow\alpha}^{II}, \quad (8)$$

in terms of the modified Green's functions $g_{i+\delta\uparrow}^{II}$ at the other sublattice, and

$$g_{i+\delta\uparrow\alpha}^{II} = \frac{\delta_{\alpha+}}{\omega - \Lambda_{i+\delta\uparrow}^{II\alpha}}, \quad (9)$$

where Λ are the self energies of the new Green's functions g , which are given in turn by:

$$\Lambda_{i+\delta\uparrow}^{II\alpha} = \sum_{\delta'} t_{i+\delta,i+\delta+\delta'}^2 g_{i+\delta+\delta'\uparrow\alpha}^I, \quad (10)$$

and,

$$g_{i+\delta+\delta'\uparrow\alpha}^I = \frac{\delta_{\alpha+}}{\omega - \Lambda_{i+\delta+\delta'\uparrow}^{I\alpha}}, \quad (11)$$

$$\Lambda_{i+\delta+\delta'\uparrow}^{I\alpha} = \sum_{\delta''} t_{i+\delta+\delta', i+\delta+\delta'+\delta''}^2 g_{i+\delta+\delta'+\delta''\uparrow\alpha}^{II}, \quad (12)$$

etc.

At this point a further approximation is necessary: we take ensemble average over all possible local spin configurations and we define the magnetization m to characterize the background of localized spins at the lattice sites. Thus, we introduce the probability $\nu_\alpha = (1 + \alpha \cdot m)/2$ that a site has parallel ($\alpha = +$) or antiparallel ($\alpha = -$) localized spin to the quantization axes in each sublattice and we write:

$$G_\alpha^I = \frac{\nu_\alpha}{\omega - \Delta^{I\alpha}}, \quad (13)$$

$$\Delta^{I\alpha} = (k+1)t^2(\cos^2(\theta)g_\alpha^{II} + \sin^2(\theta)g_{-\alpha}^{II}), \quad (14)$$

$$G_\alpha^{II} = \frac{\nu_\alpha}{\omega - \Delta^{II\alpha}}, \quad (15)$$

$$\Delta^{II\alpha} = (k+1)t^2(\cos^2(\theta)g_\alpha^I + \sin^2(\theta)g_{-\alpha}^I), \quad (16)$$

$$g_\alpha^{II} = \frac{\nu_\alpha}{\omega - \Lambda^{II\alpha}}, \quad (17)$$

$$\Lambda^{II\alpha} = k t^2 (\cos^2(\theta)g_\alpha^I + \sin^2(\theta)g_{-\alpha}^I), \quad (18)$$

$$g_\alpha^I = \frac{\nu_\alpha}{\omega - \Lambda^{I\alpha}}, \quad (19)$$

$$\Lambda^{I\alpha} = k t^2 (\cos^2(\theta)g_\alpha^{II} + \sin^2(\theta)g_{-\alpha}^{II}), \quad (20)$$

Eliminating the self-energies and using the symmetry between lattices I and II the former equations can be reduced to two interconnected equations:

$$g_+ = \frac{\nu_+}{\omega - k t^2 (\cos^2(\theta) g_+ + \sin^2(\theta) g_-)}, \quad (21)$$

$$g_- = \frac{\nu_-}{\omega - k t^2 (\cos^2(\theta) g_- + \sin^2(\theta) g_+)}, \quad (22)$$

from which we finally obtain:

$$G_\alpha = \frac{\nu_\alpha}{\omega - (k+1)t^2 (\cos^2(\theta) g_\alpha + \sin^2(\theta) g_{-\alpha})}, \quad (23)$$

where $(k+1)$ is the number of nearest neighbors (six for the simple cubic Mn lattice).

Solving Eqs. 21 to 23 allow us to obtain the densities of states per site $\rho(m, \theta, \omega) = \rho_+(m, \theta, \omega) + \rho_-(m, \theta, \omega)$, with

$$\rho_\pm(m, \theta, \omega) = \text{Im}(G_\pm)/\pi. \quad (24)$$

For $m = 0$, we obtain the paramagnetic case: $G_- = G_+$ given by

$$G_+ = \frac{0.5}{\omega - \frac{(k+1)}{2k} (\omega + \sqrt{\omega^2 - 2kt^2})}. \quad (25)$$

As expected, we see that G_\pm is independent of the canting angle and the band-width reduces to $(2\sqrt{2kt^2})$.

For $m = 1$, the extreme order case occur: $G_- = 0$ and G_+ reduces to

$$G_+ = \frac{1}{\omega - \frac{(k+1)}{2k} (\omega + \sqrt{\omega^2 - 4kt^2 \cos^2(\theta)})}, \quad (26)$$

this Eq. shows that the maximum band-width occur for the ferromagnetic case ($\theta = 0$), this is in agreement with the result of Ref. [9]. For $\theta = \pi/2$, we obtain the antiferromagnetic case and the density of states reduces to the delta function.

For $0 < m < 1$, Eq.24 shows two different pictures according to the canting angle θ :

a) for $\pi/2 \geq \theta \geq \pi/4$, we have a density of states with a central one and two lateral bands as shown in Fig. 1.

b) for $\pi/4 \geq \theta \geq 0$, we have a single band structure similar to the ferromagnetic case obtained in ref. [11] and the band-width decrease with θ . We show this band structures in Fig. 2.

The density of states allows us to write x as:

$$x = \int_{-\infty}^{\varepsilon_F} \rho(m, \theta, \omega) d\omega. \quad (27)$$

For a fixed value of doping x , Eq. 27 determine the Fermi energy ε_F . Henceforth, we take $k = 5$ and the hopping energy $t = 1$.

The kinetic energy is given by

$$E_{kin}(m, \theta, x) = \int_{-\infty}^{\varepsilon_F} \rho(m, \theta, \omega) \omega d\omega. \quad (28)$$

For $x = 0.5$, E_{kin} has the lowest energy.

In order to obtain the magnetization and the canted angle as a function of temperature we need to calculate the free energy. To this purposes, we can write the following expression for the free energy:

$$F = E_{kin}(m, \theta, x) + E_K(m, \theta, K) - T \cdot S(m), \quad (29)$$

where $E_K(m, \theta, K)$ is the antiferromagnetic superexchange energy related to the localized spins and given in mean field approximation by:

$$E_K(m, \theta, K) = Km^2 \cos(2\theta), \quad (30)$$

and $S(m)$ is the entropy term, and we take the simplest possible form compatible with our earlier approximations:

$$S(m) = \ln(2) - \nu_+ \ln(2\nu_+) - \nu_- \ln(2\nu_-). \quad (31)$$

More accurate forms of the entropy valid in the mixed valence regime can be used, see for example [21].

In Eq.29 m and θ take the values corresponding to the minimum of F for a given x , K , and T ($t = 1$ is the unit of energy).

At zero temperature, the phase diagram is dominated by the competition between the DE mechanism and the superexchange energy. For $K \ll t$, the kinetic energy is the most important term in the ground state energy and the minimum correspond to $m = 1$ and $\theta = 0$ which define the ferromagnetic phase (F). For $K \gg t$, the relevant term emerges from the superexchange interactions and the minimum correspond to $m = 1$ and $\theta = \pi/2$ which

define the antiferromagnetic phase (AF). When K and t have the same order, competition between both energies take place and a phase which we call pseudo spin glass (PSG), defined by $m < 1$, appears. We obtain two different PSG phases according to the value of K/t . So that, starting from the F phase and increasing K we obtain first a ferromagnetic pseudo spin glass (FPSG) characterized by $\theta = 0$, and then a second transition into an antiferromagnetic pseudo spin glass (AFPSG) with $\theta = \pi/2$. Finally, starting from the AFPSG and increasing K we observe the canted phase (C), where the minimum corresponds to $m = 1$ and $\theta < \pi/2$ (as K increases, $\theta \rightarrow \pi/2$). Figures 3 and 4 show this behaviour for two values of the concentration. PSG phases reduce with x and disappear for $x = 0.5$ as shown in Fig. 4.

The presence of the PSG phases, both in the ferro and antiferromagnetic regimes suggests that the competition between DE and SE interactions gives rise to frustration rather than to the canted state. This differ from the results obtained by Arovas and Guinea [27] who used a Schwinger boson formalism to describe hole doped LaMnO₃. However, the phase diagram obtained here, is very similar to that obtained by Golosov et.al. [28] . Both, this treatment and ours, allow for local distortions of the spin arrangement to lower the kinetic energy of itinerant electrons, we think that the PSG state is a state were local distortions appear in the ferro or antiferro magnetic phases.

At finite temperature, the phase diagrams can be obtained in a straightforward way from the free energy F .

For small antiferromagnetic interaction ($K \ll t$), starting in the F phase and increasing the temperature T we find a second order transition into the paramagnetic phase (P), stable at high temperature and defined by $m = 0$ at any value of θ (the free energy is independent of θ). For large antiferromagnetic coupling ($K \gg t$), starting in the AF phase and increasing T we obtain again a second order transition into the paramagnetic phase (P). In either case, a linear dependence of the critical temperature (T_c) is obtained: $T_c \rightarrow \pm 2K$ for $K/t \rightarrow \infty$.

When K and t are the same order, the competition between both take place and different transitions can occur increasing T at low temperatures:

a) Starting from the C phase we obtain a first order transition into AF phase. We show these transitions in Fig. 3 and Fig. 4.

b) For small values of doping x , we obtain a first order transition from AF into F in a narrow region of the antiferromagnetic coupling. This transition is depicted in Fig. 3.

c) For x near to 0.5, at very low temperatures the phase diagram shows a second order transition from C into P. See Fig. 4.

In conclusion, we have studied the competition between double exchange mechanism for itinerant electrons and antiferromagnetic superexchange interaction for localized electrons. We approach the problem by truncating the hamiltonian to reduce the hund energy to a z component coupling and calculate Green's functions using an RPE and mean field approximation to obtain the density of states for the itinerant electrons. We have then calculated the Free energy, to obtain the different phase diagrams for different dopings. The type of magnetic order assumed makes our calculations valid only for the electron doped manganese perovskites.

Acknowledgments

One of us (R. A.) is supported by the Consejo Nacional de Investigaciones Científicas y Técnicas (CONICET). B. A. is partially supported by CONICET.

REFERENCES

- [1] R. von Helmholt, J. Wecker, B. Holzapfel, L. Schultz, and K. Samwer, Phys. Rev. Lett. **71**, 2331 (1993).
- [2] G. H. Jonker and J. H. van Santen, Physica **16**, 337 (1950); J. H. van Santen and G. H. Jonker, Physica **16**, 599 (1950).
- [3] C. Zener, Phys. Rev. **82**, 403 (1951).
- [4] P. W. Anderson and H. Hasegawa, Phys. Rev. **100**, 675 (1955).
- [5] P. G. de Gennes, Phys. Rev. **118**, 141 (1960).
- [6] K. Kubo and N. Ohata, J. Phys. Soc. Jpn. **33**, 21 (1972).
- [7] J. Mazzaferro, C. A. Balseiro, and B. Alascio, J. Phys. Chem. Solids **46**, 1339 (1985).
- [8] Y. Moritomo, A. Asamitsu, and Y. Tokura, Phys. Rev. B **51**, 16491 (1995); Y. Okimoto, T. Katsufuji, T. Ishikawa, A. Urushibara, T. Arima, and Y. Tokura, Phys. Rev. Lett. **75**, 109 (1995); S. W. Cheong, H. Y. Hwang, P. G. Radaelli, D. E. Cox, M. Marezio, B. Batlogg, P. Schiffer, and A. P. Ramirez, Proceedings of the "Physical Phenomena at High Magnetic Fields - II" Conference, Tallahassee, Florida. World Scientific, to be published;; M. C. Martin, G. Shirane, Y. Endoh, K. Hirota, Y. Moritomo, and Y. Tokura, To be published; R. Mahendiran, R. Mahesh, A. K. Raichaudhuri, and C. N. R. Rao, Solid State Commun. **94**, 515 (1995); H. L. Ju, J. Gopalakrishnan, J. L. Peng, Qi Li, G. C. Xiong, T. Venkatesan, and R. L. Greene, Phys. Rev. B **51**, 6143 (1995); M. K. Gubkin, A. V. Salesskii, V. G. Krivenko, T. M. Perekalina, T. A. Khimich, and V. A. Chubarenko, JETP Lett. **60**, 57 (1994).
- [9] N. Furukawa, J. Phys. Soc. Jpn. **63**, 3214 (1994).
- [10] A. J. Millis, P. B. Littlewood, and B. I. Shraiman, Phys. Rev. Lett. **74**, 5144 (1995).
- [11] R. Allub and B. Alascio, Solid State Commun. **99**, 613 (1996); R. Allub and B. Alascio,

- Phys. Rev. B **55**, 14113 (1997).
- [12] E. O. Wollan and W. C. Koehler, Phys. Rev. **100**, 545 (1955).
- [13] J. Briático, B. Alascio, R. Allub, A. Butera, A. Caneiro, M. T. Causa, and M. Tovar, Phys. Rev. B **53**, 14020 (1996).
- [14] E. Müller-Hartmann and E. Dagotto, to appear in PRB, cond-mat/9605041.
- [15] Y. Tokura, A. Urushibara, Y. Moritomo, T. Arima, A. Asamitsu, G. Kido, and N. Furukawa, J. Phys. Soc. Jpn. **63**, 3931 (1994).
- [16] See, e.g., E. N. Economou, *Green's Functions in Quantum Physics* Springer Series in Solid-State Sciences **7**, Ed. P. Fulde.
- [17] P. W. Anderson, Phys. Rev. **109**, 1492 (1958).
- [18] D. C. Licciardello and E. N. Economou, Phys. Rev. **11**, 3697 (1975).
- [19] P. Lloyd, J. Phys. C **2**, 1717 (1969).
- [20] J. M. Ziman, J. Phys. C **2**, 1230 (1969).
- [21] A. A. Aligia Thesis, Instituto Balseiro (1984).
- [22] N. F. Mott and E. A. Davis, *Electronic Processes in Non-Crystalline Materials*, Oxford University Press (1971).
- [23] H. Y. Hwang, S.W. Cheong, P. G. Radelli, M. Marezio, and B. Batlogg, Phys. Rev. Lett. **75**, 914 (1995).
- [24] H. Kuwahara, Y. Tomioka, A. Asamitsu, Y. Moritomo, Y. Tokura, Science **270**, 961 (1995).
- [25] Guo-meng Zhao, K. Conder, H. Keller and K. A. Muller, Nature **381**, 676, (1996).
- [26] J. Briático, B. Alascio, R. Allub, A. Butera, A. Caneiro, M. T. Causa, and M. Tovar.

Czechoslovak J. Phys. **46**, S4 2013 (1996).

[27] D. P. Arovas and F. Guinea, preprint

[28] D. I. Golosov, M. R. Norman, and K. Levin, cond-mat/9712094

FIGURE CAPTIONS

Figure 1. Total density of states versus energies (ω) for $k/t = 5$, $m = 0.9$, and two different values of the canting angle in the region $\pi/4 \leq \theta \leq \pi/2$. The "side" bands are related with a process of hopping electron between a localized spin oriented parallel to its direction of quantization (+) and a first neighbor localized spin oriented antiparallel to its corresponding quantization direction (-).

Figure 2. Total density of states as a function of ω for $k/t = 5$, $m = 0.9$, and two different values of the canting angle in the region $0 \leq \theta \leq \pi/4$.

Figure 3. Phase diagram T/t vs K/t , with a $x = 0.1$ electrons/site. Different phases appears: paramagnetic (P), ferro (F), antiferro (AF), canted (C) and pseudo spin glass (FPSG and AFPSG). Transitions into the P phase are second order. All others transitions are first order.

Figure 4. Phase diagram T/t vs K/t , with a $x = 0.5$ electrons/site. For this concentration, the kinetic energy is the lowest and then the PSG phases disappear. We can see paramagnetic (P), ferro (F), antiferro (AF), and canted (C) phases only. Transitions into the P phase are second order. All others transitions are first order. Note the interphase between F and C phases.

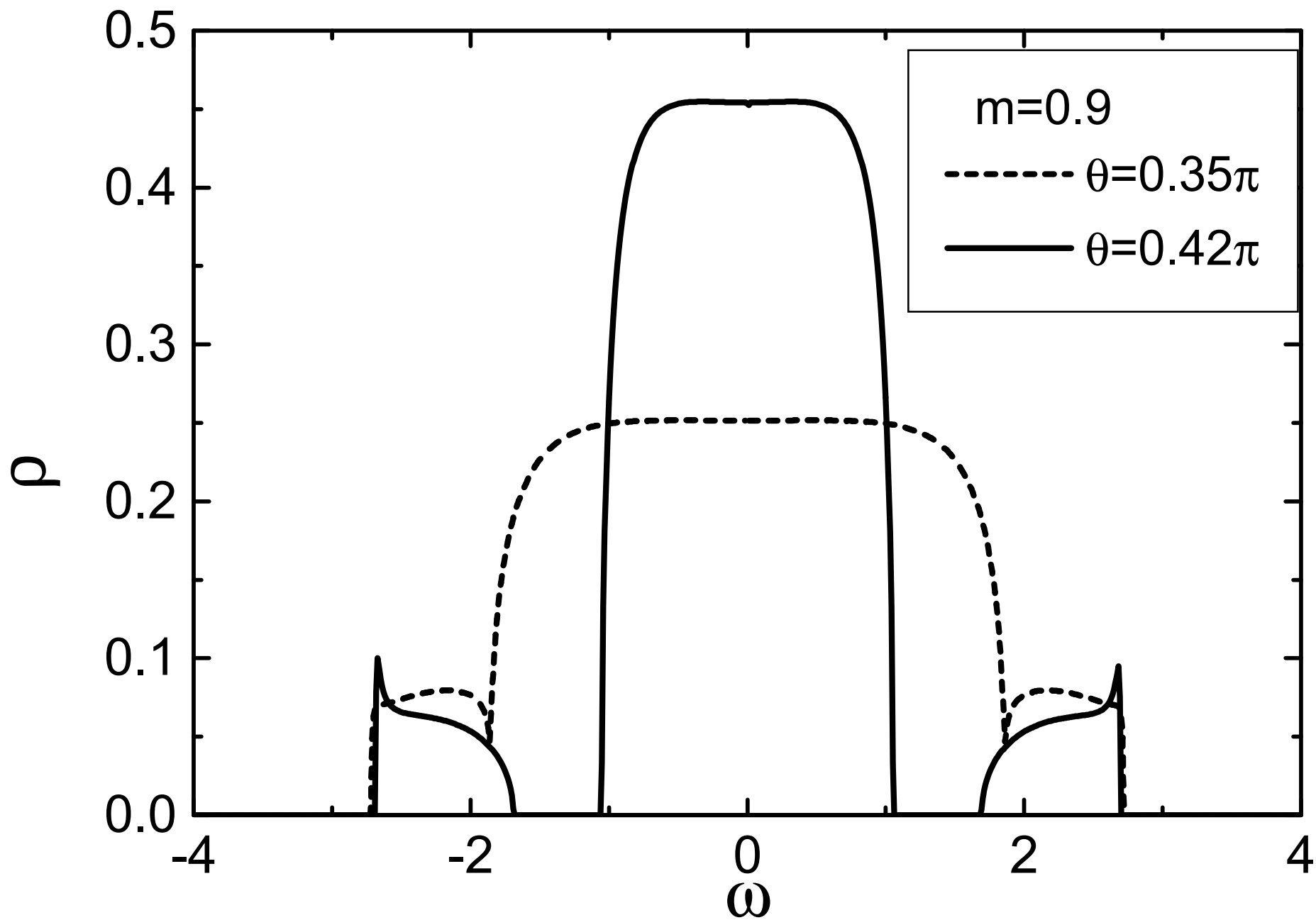


Fig 1. Aliaga et. al

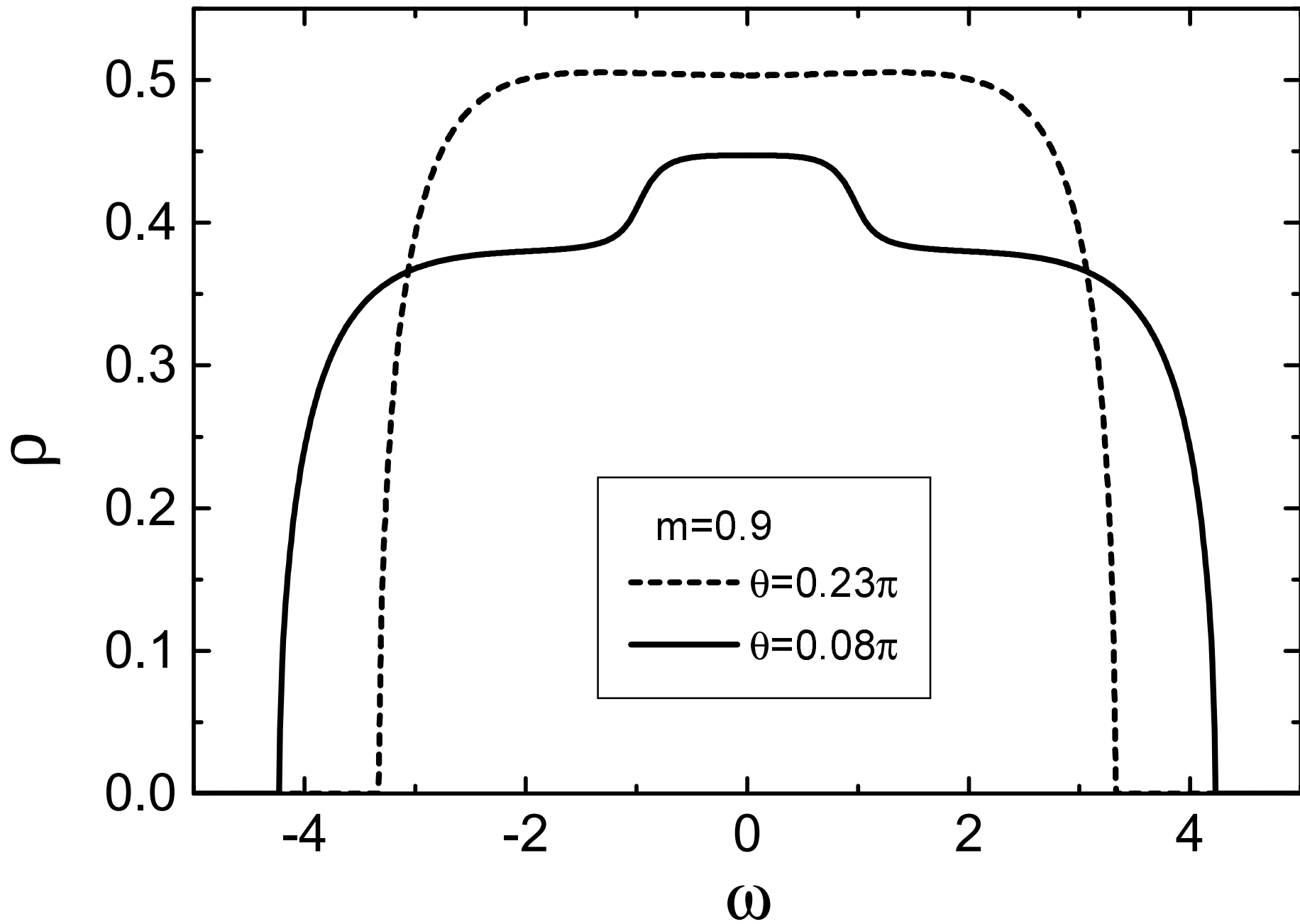


Fig. 2 Aliaga et al.

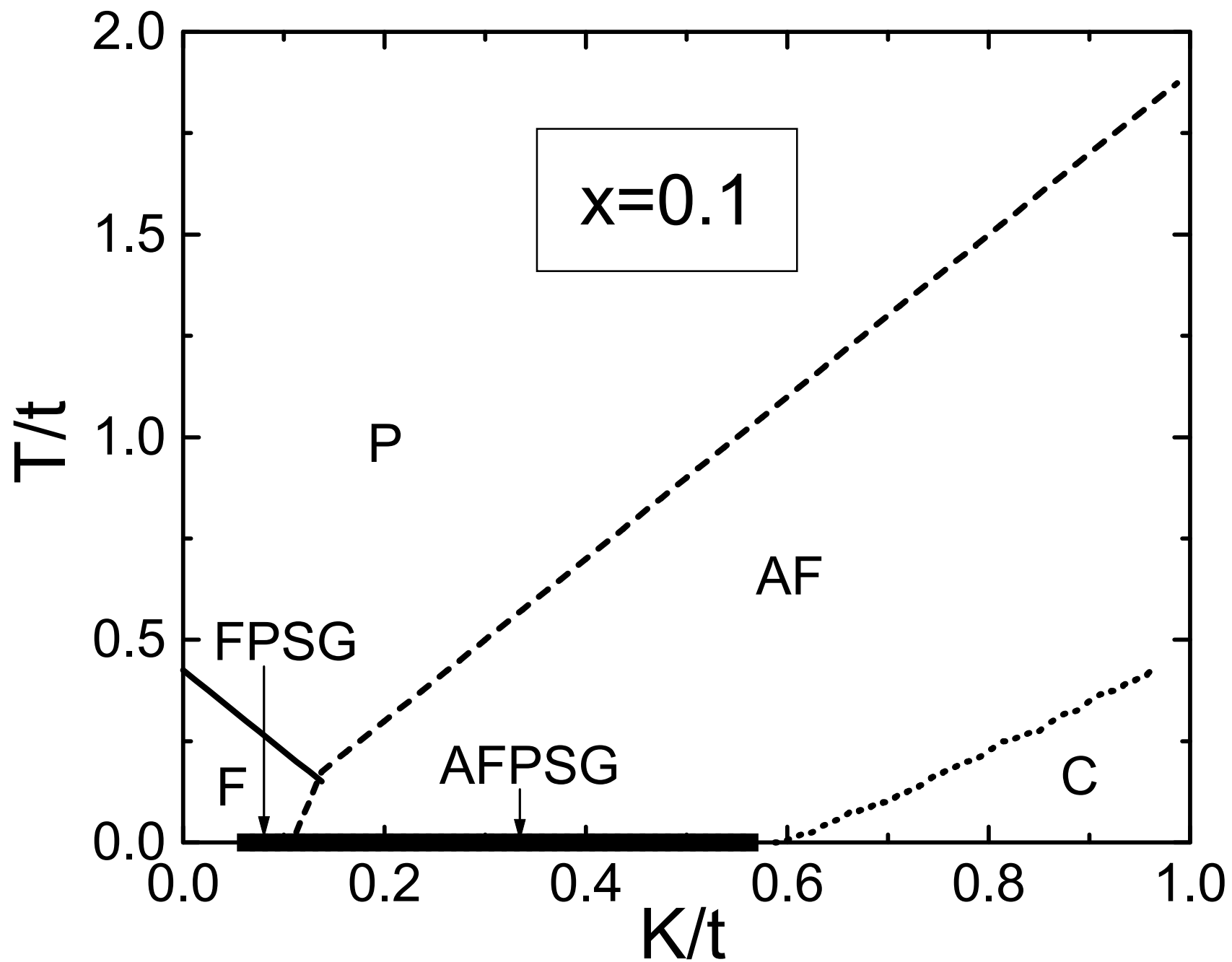


Fig. 3 Aliaga et al.

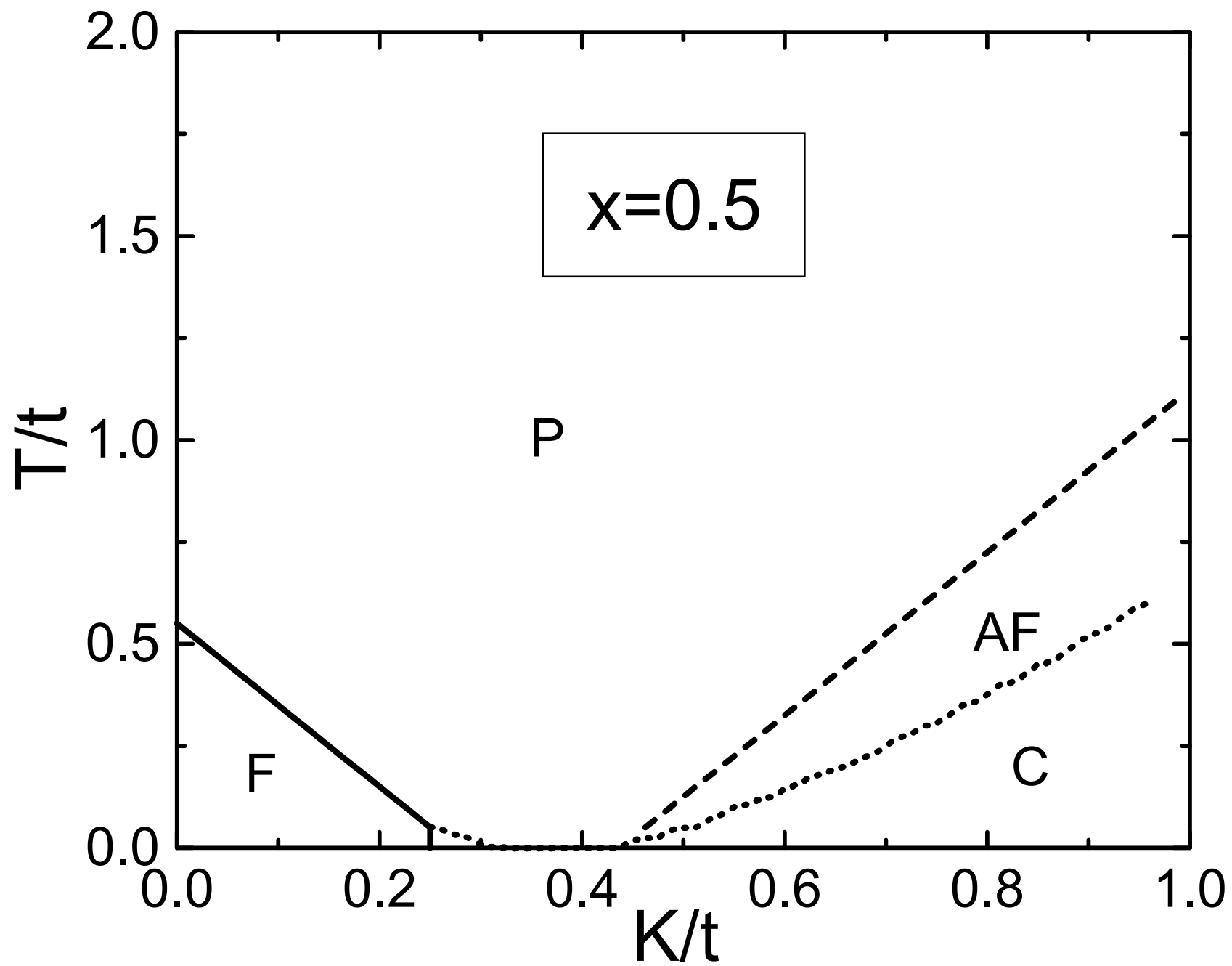


Fig. 4 Aliaga et al.